Dynamic and Static Performance Analysis of SiC MOSFET with PWM Control

Yue Qiu[1], En Fang[1,2](✉), and Delu Li[3]

[1] School of Electrical and Control Engineering,
Xuzhou University of Technology, Xuzhou 221018, Jiangsu, China
`fangen@cumt.edu.cn`
[2] Jiangsu Key Construction Laboratory of Large Engineering Equipment Testing and Control Technology, Xuzhou 221018, Jiangsu, China
[3] Jiangsu Vocational Institute of Architecture Technology, Xuzhou 221018, Jiangsu, China

Abstract. The superior electrical and thermal properties of silicon carbide (SiC) power electronic devices, compared with silicon (Si) devices, lead to high efficiency and low volume in power converter designs. In this paper, the simulation model of the SiC MOSFETs is built, and the dynamic and static performance is obtained. The switching loss of SiC devices for AC motor control with pulse width modulation is calculated and analyzed.

Keywords: SiC MOSFET · Switching loss

1 Introduction

In the development of power electronic technology, power electronic devices (power devices) are the decisive factors to promote the development of power electronic technology. Although the value of power electronic devices in the whole machine is not high (10%–30%), the quality of power electronic devices directly determines the performance of the entire device. It can be said that the performance index of power electronic devices directly determines the performance index of equipment.

Since the first electron tube came out in 1904, the technology for power conversion has existed. It was not until 1957 that GE developed the first thyristor, which marked the birth of power electronics technology and the first technological revolution in the electrical age. In the 60 years since then, the power electronic technology has been continuously improved, and the performance of power devices has been gradually improved.

1.1 Development of Power Electronic Devices

The development of power semiconductor devices has experienced three stages.

The First Generation: SCR and Its Derivatives. The thyristor is a semi-controlled device, which can be turned on but not off by controlling the gate. The control mode

D. Jiang and H. Song (Eds.): SIMUtools 2021, LNICST 424, pp. 331–341, 2022.
https://doi.org/10.1007/978-3-030-97124-3_25

of the thyristor circuit is mainly phased control mode. The thyristor is used to realize large capacity current control in low-frequency phase control. However, the working frequency of the thyristor is limited by d*v*/d*t* and d*i*/d*t*, so thyristor is mainly used at a low switching frequency.

At present, in the field of superpower (voltage above 3.3 kV, capacity within 1–45 MW), thyristors and other power devices have a considerable market. Thyristors of 6-inch substrate with 8.5 kV/5 kA have been commercialized in the world. ABB and other companies in Switzerland have developed IGCT products with asymmetric structure, reverse conduction or reverse resistance. As 4.5 kV and 6 kV series products have been commercialized in the market, and 6.5 kV/6 kA series products have been supplied, the 9 kV/6 kA series products are researched and developed.

Second Generation: Power MOSFETs. In the late 1970s, GTO, BJT, and MOSFET devices developed rapidly. Through the control of the gate (base, gate) to turn it on or off. Especially for MOSFET, its driving circuit is simple, and it needs small driving power, fast switching speed, and high working frequency. Therefore, power MOSFET can work at a higher frequency and has a much wider safe working area than thyristor.

However, power MOSFET has a small current capacity and low withstand voltage, so there are not many applications of power MOSFET in large capacity and high power environments. In the field of medium and small power (below 900V), power MOSFET is still the device with the largest market capacity and the fastest-growing demand. The new structure device represented by super junction is the critical development direction of the device.

At the same time, since the 1990s, technology-leading enterprises have focused on wide bandgap semiconductor devices represented by SiC and GaN.

The Third Generation: IGBTs. GTO and other bipolar devices have a solid current capacity, but the switching speed is slow. The driving power required is enormous, and the driving circuit is complex. The switching speed of power MOSFET is fast, and the driving power is small. And the driving course is simple. Therefore, in 1982, GE proposed designing and developing a fully controlled power device, i.e., insulated gate bipolar transistor, which has the advantages of both MOSFET and bipolar device.

Due to the excellent characteristics of IGBT, it has become the leading device of medium and high power (voltage 1200 V–6.5 kV) for power electronic equipment. At present, IGBT devices have covered the field of 300 V–6.5 kV and 2 A–3600 A.

1.2 Development and Application of SiC Materials

Since the first generation of power devices, Si and Ge have been widely used as semiconductor materials. With the rapid development of technology, power devices based on Si, GaAs, and other traditional semiconductor materials have been developed. The corresponding technology has reached its limit. However, traditional materials such as Si and GaAs are facing severe challenges when working in extreme environments. Firstly, the low dielectric breakdown field of Si limits the maximum operating voltage of power devices, and the narrow bandgap and low thermal conductivity of Si lower the maximum operating temperature of power devices. Therefore, people urgently need a new type of material that can work stably at high temperature, high frequency, high power, intense radiation, and other extreme conditions.

Development of SiC Materials. In 1824, Swedish scientist Berzelius observed SiC in the process of synthetic diamond, which marked the beginning of SiC research. In 1885, Acheson first produced SiC crystal by hand and found that the crystal had high hardness and a high melting point. SiC material was hoped to be used as abrasive material, and the method of artificial preparation of SiC crystal was also named as Acheson method. In 1891, industrial SiC was successfully developed and became the earliest man-made abrasive. In 1907, a British engineer named Round produced the first light-emitting diode made of SiC, marking the formal application of SiC in electronics. In 1920, SiC single crystal was used as a detector in the early radio receiver. In 1959, Lely improved the manufacturing process, which laid the foundation for the development of SiC. This new method of producing SiC also became Lely method. In 1978, Russian scientists Tairov and Tsvetkov improved the Lely method to obtain SiC growth technology with larger crystals. In 1979, SiC blue LED was successfully manufactured. In 1981, Matsunami invented the technology of growing single-crystal SiC on Si substrate. In 1991, Cree produced 6H-SiC wafers by the improved Lely method. In 1994, Cree obtained 4H-SiC wafers. In 1997, Cree realized the marketization of 2-inch 6H-SiC wafers. In 2000, Cree accomplished the marketization of 4-inch 6H-SiC wafers. In 2007, Cree released a commercial 100 mm SiC substrates with zero microtubes. In 2010, Cree displayed high-quality 150 mm SiC wafers. In 2013, Cree developed 6-inch SiC single crystal products. So far, Cree and Rohm have developed SiC MOSFET products with voltage levels ranging from 650V to 1700V, and the maximum single-chip current exceeds 50A. All series of SiC power module products within 1200V/300A and 1700V/225A are developed.

Physical Properties of SiC Materials. SiC, as one of the third core generation semiconductor materials, has the advantages of the wide bandgap, high thermal conductivity, small thermal expansion coefficient, high electron saturation drift rate, strong insulation breakdown field, and good wear resistance compared with Si and GaAs. Therefore, SiC can be used for manufacturing high temperature, high frequency, high power density, and radiation-resistant power electronic devices. In addition, SiC materials can form oxide layer SiO_2 on the surface naturally, which is very beneficial to MOS devices.

The third-generation wide bandgap semiconductor materials have the following advantages compared with the first generation of traditional Si materials:

(1) The gap width of SiC and Gan materials is three times that of Si materials. The large bandgap width significantly reduces the leakage current of SiC devices. SiC and Gan devices have radiation resistance properties, which can improve the service life in extreme environments. Secondly, different crystalline states have other band gaps, which can be used as luminescent materials of various colors.

(2) SiC materials are of high thermal conductivity, which leads to excellent heat dissipation, and helps to improve the power density and integration of the devices. In addition, the high-temperature resistance of SiC materials also makes it have a unique advantage in a high-temperature environment. Theoretically, the junction temperature of SiC devices can work around 600 °C, which is far greater than the operating temperature range of Si.

(3) The insulation breakdown field of SiC is higher than that of Si material, which dramatically improves the voltage withstand capacity and current density of SiC devices. At the same time, the on-resistance of power semiconductors is inversely proportional to the cubic of the breakdown field strength, so the on-resistance of SiC is smaller, and the conduction loss is lower.

(4) The electron drift rate of SiC is twice as high as that of Si. SiC devices have excellent microwave characteristics and can work at higher frequencies and meet particular environments such as aerospace.

It can be seen that the wide bandgap semiconductor material has the incomparable advantages of Si materials. The power devices made by wide bandgap material can meet particular environmental requirements and meet the development needs of power electronic devices better, such as high temperatures, high voltage, and high-power density.

2 Characteristic Analysis of MOSFETs Based on SiC

Based on the advantages of SiC materials, the SiC semiconductor devices have the benefits of low on-resistance, high breakdown voltage, and high limit operating temperature. By comparing the output characteristics and switching characteristics of Si devices and SiC devices, the advantages of SiC devices are analyzed and compared.

2.1 Essential Characteristics of Power MOSFETs

Static Characteristic. The relationship between drain DC I_{D} and gate-source voltage U_{GS} reflects the relationship between the input voltage and output current, also known as the transfer characteristics of MOSFET, as shown in Fig. 1. And the slope of the curve is defined as the transconductance G_{FS} of MOSFET.

$$G_{\mathrm{fs}} = \frac{\mathrm{d}I_D}{\mathrm{d}U_{GS}}$$

Figure 2 shows the volt-ampere drain characteristics of power MOSFET, i.e., output characteristics. Like a thyristor, the power MOSFET also has three working regions: cut-off, unsaturated, and saturated regions. In the saturated area, the drain current does not increase with the increase of drain-source voltage, while in the unsaturated region, the drain current increases with the rise of drain-source voltage. The working state of MOSFET switches back and forth between the cut-off region and the unsaturated region.

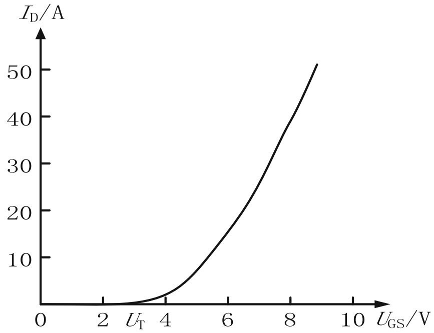

Fig. 1. Transfer characteristics of power MOSFETs.

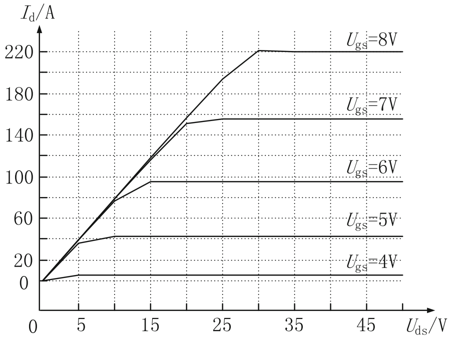

Fig. 2. Output characteristics of power MOSFETs.

Dynamic Characteristics. Figure 3 shows the dynamic characteristics of power MOSFET, which is the voltage and current waveforms during switching. There is inter junction capacitance in power MOSFETs, so when the rising edge of the switching pulse comes, the gate-source voltage U_{GS} will rise exponentially. When the U_{GS} rises to threshold voltage U_{th}, the drain current I_D appears. After that, the drain current I_D increases with the rise of gate-source voltage U_{GS}. When the drain current rises to the steady-state, the gate voltage rises to U_{gsp}, and the drain voltage U_{DS} begins to decline. During the process of the drain voltage U_{DS} falling, the grid voltage U_{GS} will be maintained at the value of U_{gsp} and form a platform called the Miller platform. It will not continue to rise to the steady-state value in exponential form until the end of the drain voltage drop.

Miller platform is formed because the gate signal reversely charges the capacitance between gate-drain during voltage drop time, and the size of U_{gsp} is related to the steady-state value of I_D.

The opening delay time of power MOSFET is described as follows.

$$T_{on} = T_{d(on)} + T_{ri} + T_{fv}$$

Where, the turn-on delay time T_{on} refers to the time from the gate-source voltage U_{GS} from 0 to the drain current I_D. T_{ri} is the current-rise time, which refers to how long the drain current I_D rises from 0 to the steady-state value. T_{fv} refers to the time during which the drain voltage begins to drop to 0.

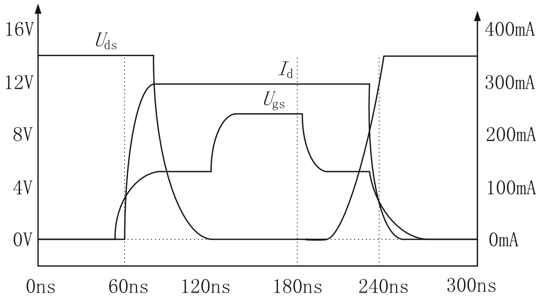

Fig. 3. Dynamic characteristics of power MOSFETs.

The turn-off process of power MOSFET is opposite to the turn-on process, including turn-off delay time $T_{d(off)}$, voltage rise time $T_{rv,}$ and current fall time T_{fi}.

$$T_{off} = T_{d(off)} + T_{rv} + T_{fi}$$

2.2 Modeling and Characteristic Analysis of SiC MOSFET

Modeling of SiC MOSFETs Based on MATLAB/Simulink. Based on the equivalent structure of SiC MOSFETs mentioned above, the physical model can be comparable to the circuit in Fig. 4.

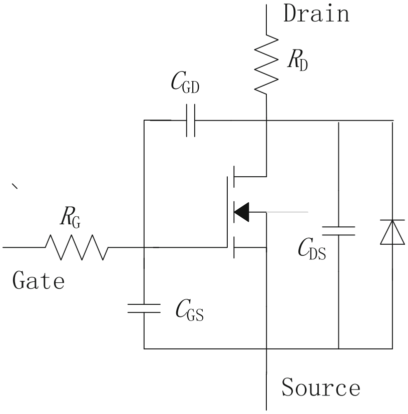

Fig. 4. Equivalent circuit of SiC MOSFETs.

The switching process of SiC MOSFET is modeled by MATLAB/Simulink. There is already a model of MOSFET in the Simulink library, but the model is an ideal model, and the characteristics of the switching process of the device can not be observed. Therefore, the equivalent simulation model of SiC MOSFET is rebuilt according to the identical circuit model, as shown in Fig. 5.

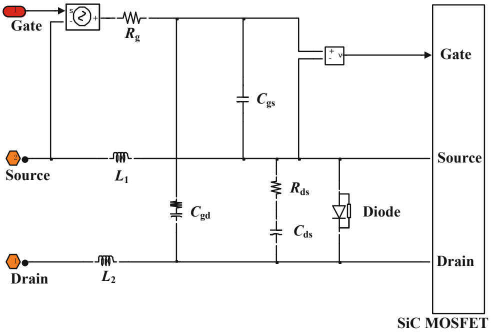

Fig. 5. Equivalent simulation model of SiC MOSFETs.

In this simulation model, the inter-electrode capacitance is modeled by three capacitor modules, and the body diode is modeled by a diode. For the on-off characteristics of MOSFET, the reverse layer is modeled by a controllable current source, as shown in Fig. 6.

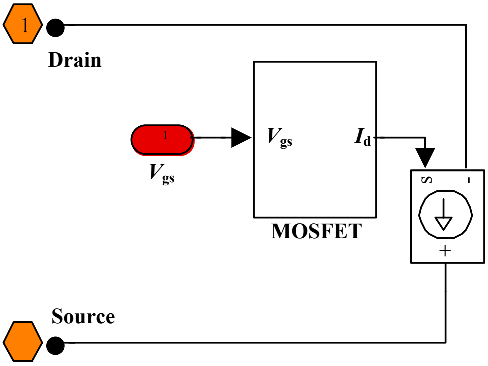

Fig. 6. Equivalent simulation model of the inversion layer in SiC MOSFETs.

The input of the module is gate-source voltage, and the output is the drain current. The output current is directly converted into the ideal current, which is output by a controllable current source, and its transfer function is written as follows.

$$I_\mathrm{d} = K_\mathrm{n}(V_\mathrm{GS} - V_\mathrm{DS})^2$$

The whole simulation model is shown in Fig. 7. The MOSFET model is placed in the half-bridge, and a diode replaces the upper half-bridge device. The switching characteristics of SiC MOSFET model are analyzed by the dual-pulse test method.

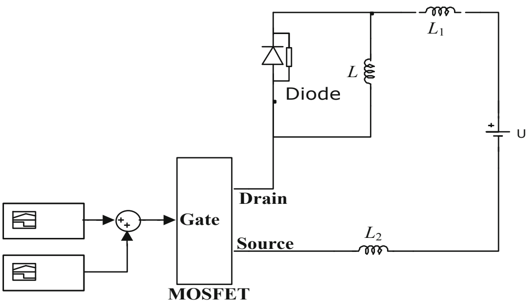

Fig. 7. Simulation model of dual-pulse test for SiC MOSFETs.

Figure 8 shows the waveforms of gate-source voltage, drain-source voltage, and drain current during the turn-on process. In the initial state, the device is turned off. When 2.59 ns, the gate-source voltage increases until the drain current appears when the driving voltage is higher than the threshold voltage. At this time, the drain current increases exponentially, and the corresponding drain voltage decreases rapidly. This process is the turn-on process of MOSFET.

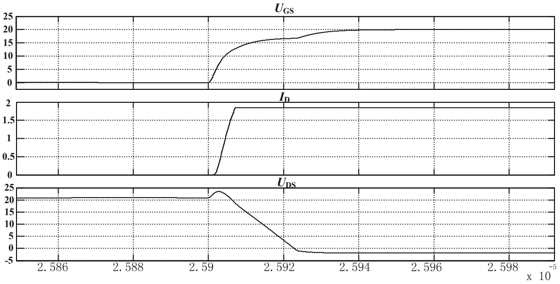

Fig. 8. Simulation waveforms of turn-on characteristics of SiC MOSFETs.

Although the MOSFET model of SiC is built by an equivalent model, the simulation waveforms are similar to the theoretical waveforms. The comparison between the model and the actual model is still insufficient, for example, the influence of junction temperature and shell temperature on the characteristics of the device can not be reflected in this model. Therefore, to observe the opening features of SiC MOSFET, it is necessary to use other software to simulate it more accurately.

3 Analysis of Dynamic Loss of SiC MOSFETs

3.1 Influence of Parasitic Inductance on Dynamic Parameters of Switching Process

Considering all the parasitic parameters in the current path, the whole loop inductance can be equivalent to three lumped inductors.

(1) The parasitic inductance L_g is formed by the gate current circuit, which mainly includes the inductance L_{g1} brought by the device packaging and the inductance L_{g2} of the external gate path of the device, which can be expressed as $L_g = L_{g1} + L_{g2}$.
(2) The parasitic inductance L_d of the power circuit is formed by the drain current path. It mainly includes MOS tube package inductor L_{d1}, PCB wiring inductor L_{d2}, upper half-bridge turn-on package inductor L_{d3}, positive and negative bus inductors L_{b1} and L_{b2}, which can be expressed as $L_d = L_{d1} + L_{d2} + L_{d3} + L_{b1} + L_{b2}$.
(3) The common source inductance L_S, which exists in two loops, connects the grid and power loops.

Influence of Parasitic Inductance of Grid Circuit on Switching Process. The gate loop inductor has only a slight effect on the switching characteristics of SiC MOSFET, and the overshoot of voltage and current remains unchanged. For the switching loss, the increase of L_g hardly affects the switching loss. Figure 9(a) shows the turn-on waveform when $L_g = 0.1\text{nH}$, and Fig. 9(b) shows the turn-off waveform when $L_g = 0.1\text{nH}$.

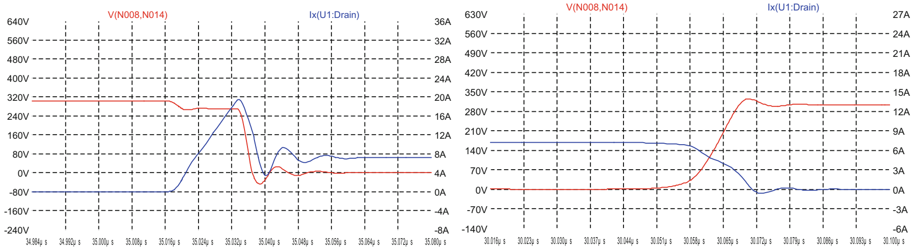

(a) Turn-on waveforms (b) Turn-off waveforms

Fig. 9. Drain- source voltage and drain current waveforms when $L_g = 0.1$ nH.

The overshoot voltage ratio calculated from the turn-off waveform is $\sigma_1 = 7.2\%$ and for current is $\sigma_2 = 171\%$ when the device is turned on. The turn-on loss is $E_{on} = 51.585\ \mu\text{J}$. And the turn-off loss is $E_{off} = 7.791\ \mu\text{J}$.

4 Conclusion

The 1.2 kV SiC MOSFET in a three-phase inverter is studied in this paper by simulation with MATLAB/Simulink in order to evaluate the loss and efficiency under different switching frequencies.

At the low switching frequency, conduction loss is the primary source of total converter loss. Even at the lowest switching frequency, the performance of SiC MOSFET is better than that of Si IGBT.

With the increase of switching frequency, the advantage of using SiC MOSFET becomes more apparent because it has lower switching loss than Si IGBT. According to the switching resistance R_g, the switching loss of Si in inverters is 1.55 to 4.79 × (25 °C) and 3.5 to 8.6 × (125 °C) that of SiC. Therefore, the switching frequency of the inverter can be increased by 1.56 to 5 times for the same output power by using SiC power devices.

The switching phenomenon of MOSFET is almost independent of the operating temperature, while the temperature dependence of Si IGBT is strong. The simulation results show that the efficiency difference between inverters can reach 5.47% when the switching frequency is 100 kHz, and the junction temperature is 25 °C. Significantly, the reverse recovery current of Si diode and the trailing current of IGBT deteriorate with the increase of temperature.

Therefore, there are many ways to optimize the circuit design to reduce the switching loss, such as improving the efficiency and reducing the cooling requirements. Most importantly, by increasing the operating frequency, the size of passive components can be reduced to improve the power density of the system.

Acknowledgements. The authors acknowledge the Jiangsu University Natural Science Research Project (18KJB470024) and Provincial Construction System Science and Technology Project of Jiangsu Provincial Housing and Urban-Rural Construction Department (2018ZD088). This work is partly supported by the Natural Science Foundation of Jiangsu Province of China (No. BK20161165), the applied fundamental research Foundation of Xuzhou of China (No. KC17072). The authorized patents for invention are also the research and development of Jiangsu Province Industry-University-Research Cooperation Project (BY2019056).

References

1. Spagnuolo, G., et al.: Renewable energy operation and conversion schemes: a summary of discussions during the seminar on renewable energy systems. IEEE Ind. Electron. Mag. **4**(1), 38–51 (2010)
2. Zuk, P.C., Odekirk, B.: SiC impacts greening of power - understanding the differences between Silicon Carbide (SiC) and Silicon (Si) for power electronics. Power Syst. Des. Eur. 3436 (2008)
3. Wrzecionko, B., Biela, J., Kolar, J.W.: SiC power semiconductors in HEVs: Influence of junction tem- perature on power density, chip utilization and efficiency. In: 35th Annual Conference of IEEE Industrial Electronics, pp. 3834–3841 (2009)
4. Evans, T., Hanada, T., Nakano, Y., Nakamura, T.: Development of SiC power devices and modules for au- tomotive motor drive use. In: 2013 IEEE International Meeting for Future of Electron Devices, pp. 116–117 (2013)
5. Skibinski, G., Braun, D., Kirschnik, D., Lukaszewski, R.: Development in hybrid Si-SiC power modules (2006)
6. Zhang, Z., Wang, F., Tolbert, L.M., Blalock, B.J., Costinett, D.J.: Evaluation of switching performance of SiC devices in PWM inverter-fed induction motor drives. IEEE Trans. Power Electron. **30**(10), 5701–5711 (2015)
7. Zhao, T., Wang, J., Huang, A.Q., Agarwal, A.: Comparisons of SiC MOSFET and Si IGBT based motor drive systems. In: 42nd IAS Annual Meeting. Conference Record of the 2007 IEEE Industry Applications Conference, pp. 331–335 (2007)
8. Rice, J., Mookken, J.: Economics of high efficiency SiC MOSFET based 3-ph motor drive. In: Proceedings of International Exhibition and Conference for Power Electronics, Intelligent Motion, Renewable Energy and Energy Management, pp. 1–8 (2014)

9. Tiwari, S., Midtgård, O.-M., Undeland, T.M., Lund, R.: Experimental performance comparison of six- pack SiC MOSFET and Si IGBT modules paralleled in a half-bridge configuration for high temperature applications. In: 2015 IEEE 3rd Workshop on Wide Bandgap Power Devices and Applications (WiPDA), pp. 135–140 (2015)
10. Tiwari, S., Abuishmais, I., Undeland, T., Boysen, K.: Silicon carbide power transistors for photovoltaic applications. In: 2011 IEEE Trondheim PowerTech, pp. 1–6 (2011)
11. Tiwari, S., et al.: Design considerations and laboratory testing of power circuits for parallel operation of sili-con carbide MOSFETs. In: 17th European Conference on Power Electronics and Applications (EPE 2015 ECCE-Europe), pp. 1–10 (2015)
12. Agarwal, A., Singh, R., Ryu, S.-H., Richmond, J., Capell, C., Schwab, S., et al.: 600 V, 1- 40 A, schottky diodes in sic and their applications (2002)
13. Heer, D., Bayoumi, A.K.: Switching characteristics of modern 6.5kV IGBT/Diode. In: Proceedings of International Exhibition and Conference for Power Electronics. Intelligent Motion, Renewable Energy and Energy Management, pp. 1–8 (2014)
14. Cree, Inc.: SiC MOSFET Isolated Gate Driver, CPWR-AN10 Rev. C (2014)